FIELD METHODOLOGY FOR RECONSTRUCTION OF A *PINUS RADIATA* LOG

ROBERTO COMINETTI

Departamento Ingeniería and Centro de Modelamiento Matemático UMR 2071
CNRS, Universidad de Chile, Casilla 170-3, Correo 3, Santiago, Chile

FERNANDO PADILLA*

Centro de Modelamiento Matemático UMR 2071
CNRS, Universidad de Chile, Casilla 170-3, Correo 3, Santiago, Chile

and JAIME SAN MARTÍN

Departamento Ingeniería and Centro de Modelamiento Matemático UMR 2071
CNRS, Universidad de Chile, Casilla 170-3, Correo 3, Santiago, Chile

ABSTRACT

We have devised a new field methodology to collect log data necessary to develop a graphical system for 3-D spatial reconstruction of the internal and external shape of the log, based on stem and cross-sectional analysis. The methodology provides a detailed internal and external description of the stem, including the full growth history of the tree as recorded in the rings. The technique may be used to analyse both straight and swept logs, and is specially suited for studying the evolution of stem sweep when a tree has lost its verticality, due to environmental factors such as snow and wind, or through destruction of the leader. We have developed the software required to process the data and to reconstruct the development inside the tree.

Keywords: stem analysis; cross-sectional analysis; log sweep; 3-D graphical reconstruction.

INTRODUCTION

Different environmental factors may cause a stem to deviate from verticality. The factors involved act mechanically (wind, snow, soil movement), physiologically (light), or through destruction of the leader (frost, drought, animals, insects, fungi, etc.). Over time, the natural growth of the tree will tend to reduce the external appearance of these defects, although the wood quality of the deformed region will be permanently affected. When pronounced, these deviations may cause high degradation in wood products (Tsoumis 1991). Reaction wood is generally formed in xylem tissue in response to a non-vertical orientation of the stem. In conifers, this tissue is associated with eccentric radial growth and is called compression wood. The signalling pathway that controls compression wood is still not fully understood, but seems to be a gravitropic response of the tree, related to intrinsic growth directions and

---

the flow of growth hormones inside the tree (Plomion *et al.* 2000). Harris (1991) pointed out that formation of compression wood can be explained as a geotropic response to an inertial force (i.e., a growth response that strengthens the ability of the tree to resist gravity). Zimmermann & Brown (1971) also reported the importance of gravity as one of the most important formative factors in plants. Due to the continuous and uniform action of gravity, plants must constantly regulate their growth.

One of the important environmental factors that may affect stem verticality is related to alterations in the leader shoot due to the attack of different pests. Our study was in fact motivated by the presence in Chile of the European Pine Shoot Moth (*Rhyacionia buoliana* Den et Shiff.) which was first detected in 1985 and has now become an important pest of major economic impact in the forestry industry. This pest particularly attacks plantations of *Pinus radiata* D. Don. The damage is produced by larvae, which bore into terminal shoots and buds causing future stem deformation and bent stems, as well as losses in growth and wood quality (Espinoza & Inostroza 1993). The methodology described in this paper was specially conceived as a tool for studying the sweep produced in the stem as a consequence of the attack by the moth on the terminal shoot, and for investigating the evolution of these defects over time. In particular, we were interested in reconstructing a 3-D image of a pine tree and how the stem evolved in time. We observe that the vertical orientation of the stem may vary through time and this should be considered when developing models for the growth history of a tree.

In this paper we present a methodology for collecting and processing the data required to develop a 3-D digital model of the log, based on cross-sectional analysis in the spirit of Somerville's (1985) method. Taking into account the influence of gravity on growth processes, our methodology captures the original spatial orientation of the standing tree, which confers a particular characteristic of the system. A device was designed and built to establish a co-ordinate system attached to the tree, where the Z-axis is vertical. This fact is essential for studying the influence of gravity upon the tree evolution. Using this methodology, we can estimate the real spatial position of wood discs extracted from the stem, and reconstruct the internal shape of the stem based on ring information obtained from wood discs, where the data came in the form of a digitally scanned image of the disc. As a result, a detailed 3-D image of the internal and external shape of the stem is obtained, allowing the reconstruction of the full history of the tree (Padilla 2001). The digital model may be useful for studying the evolution of stem curvature and relating this to the effects of gravity.

Knowledge of the internal features of logs has had a major effect on timber quality assessment. Numerous researchers have carried out sawing method studies to find the best log orientation for highlighting defects (Peter & Bamping 1962), to obtain a detailed mapping of internal defect core and external log shape (Park & Leman 1983), or to resolve the problem between value and log yield (Steele *et al.* 1993). Others have used cross-sectional analysis to reconstruct the internal features of the log. Somerville (1985) developed a cross-sectional system, where the external and internal log features are measured in geometric co-ordinates about the central axis of the log, which is used as the Z-axis in a 3-D co-ordinate system. This co-ordinate definition of the log allows reconstruction of a 3-D image for subsequent analysis, and supports the mapping of curved stems by adding appropriate offset measurements. However, since the log axis may not coincide with the vertical direction, the effect of gravity may be lost. Harless *et al.* (1991) reconstructed the

internal features of hardwood logs using cross-sectional analysis, recording the periphery of each disc and the periphery of lumber grade defects found on each disc by means of a sonic digitiser.

Other researchers have proposed a number of techniques for detecting internal defects in logs, using non-destructive evaluation methods. These include X-ray computer tomographic (CT) imaging (Benson-Cooper *et al.* 1982; Funt & Bryant 1987; He 1997; Schmoldt 1996; Zhu *et al.* 1996), microwaves (Birkeland & Holoyen 1987), ultrasonic CT (Han & Birkeland 1992; Niemz & Kucera 1999), impulse radar (Shad *et al.* 1996), and nuclear magnetic resonance NMR (Wang & Chang 1986). Some applications of these techniques have been carried out for industrial processes. Oceña & Schmoldt (1996) developed an interactive graphic sawing program, where the data comes in the form of a CT scan and digitised co-ordinates, representing the cross-sectional profile of a log and its internal defects. Schmoldt *et al.* (1995) used tomographic X-ray scans of a log to generate data in order to simulate different veneer patterns. In a recent work, Morales *et al.* (in press) used magnetic resonance imaging (MRI) to recognise rings in *Pinus radiata* and obtain a 3-D reconstruction of logs.

In general, non-invasive methods have been used to detect defects inside the log prior to conversion, but the difficulty of using these techniques at production speeds and the high cost still limit their utilisation for industrial processes.

DESCRIPTION OF THE 3-D MEASURING DEVICE

The 3-D measuring device (3-DMD) comprises three main parts: a main structure, a holding system, and a levelling system.

The main structure consists of a rigid, U-shaped, metallic body (Fig. 1). This structure must be flat with its edges mutually perpendicular.
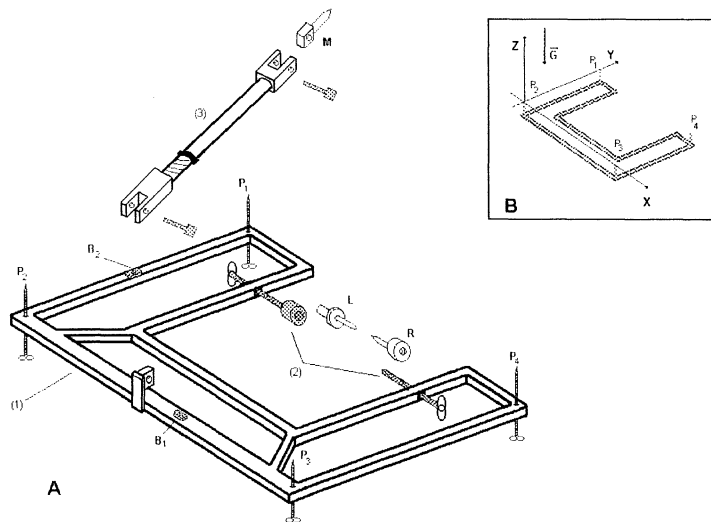

FIG. 1–(A): Description of 3-DMD. The device consists of a main structure (1), two bubble levels, three nails, a metallic arm (2), and a levelling system composed of four thin bolts. (B): The four thin bolt ends, and the vertical, establish a 3-D co-ordinate system.

The holding system consists of a right and a left nail, which are nailed into the stem and joined to the main structure through two bolts providing horizontal stability to the device. A central nail holds the main structure through a metallic arm that confers vertical stability to the system.

Four thin bolts (P_1–P_4 in Fig. 1) compose the levelling system. The bolt ends are levelled by gravity determining a horizontal plane. This plane, together with the vertical direction, provides a 3-D co-ordinate system with respect to which we may reference the position of an arbitrary point in the stem. In order to obtain a 3-D model for the log we extract a number of wood discs from the stem. Each disc will be spatially located by determining the co-ordinates of three points on its surface with respect to this reference system.

PROCEDURE AND MEASUREMENTS

The following steps describe the process of installation of the 3-DMD and the levelling of the bolts.

(1) **Determine the plane of maximum sweep.** After selecting a tree, examine the butt log for sweep. The maximal sweep plane will give the XZ-plane and the device should be installed with its longer edge parallel to this plane.

(2) **Stump height.** Mark a point with white correcting fluid on the bark at 30 to 40 cm from the ground. This mark is called the *stump mark* and indicates the first disc to be obtained from the stem. The stump mark must be placed in the maximum plane of deformation (Fig. 2). For later reference, record the height of the stump mark above the ground.
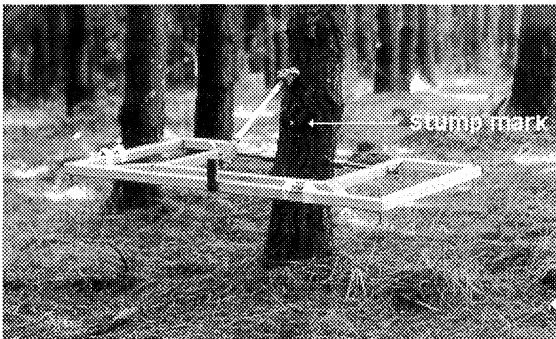

FIG. 2–Installation of 3-DMD. Note the positions of the nails with respect to the stump mark (white point). The longer axis of the device is parallel to the maximum plane of deformation.

(3) **Device installation.** Place the 3-DMD in front of the tree as mentioned in Step 1. The device should lie horizontally 10 to 20 cm below the stump mark. For later reference and to compare with the digital 3-D reconstruction, it may be useful to take a frontal picture of the tree with identification.

(4) **Levelling bolts.** Fix one of the bolts, say P_1. Adjust the other thin bolts P_2, P_3, and P_4 in such a way that their ends are levelled with respect to the end of P_1. A simple way to accomplish this task is by using a hose filled with water. The bolt ends will then provide the horizontal XY-plane.

(5) **Felling.** Take out the device and fell the tree by cutting it 10 cm below the device. Reinstall the device, recovering its original position (Fig. 3).

FIG. 3–Once reinstalled, the device recovers its original position. Photo shows the measuring process.

(6) Butt log. Make a cross-cut to obtain a 6-m butt log, and prune it throughout its length.

(7) Where to obtain the wood discs. Examine the butt log to determine the positions at which the wood discs should be extracted. The spacing between discs is a function of the local sweep of the stem and may vary from 5 to 80 cm. To obtain an accurate reconstruction of the log it is important to extract a sufficient number of discs from the swept zones. In the regions without significant deformation the distance may be longer but should not exceed 80 cm to avoid the loss of annual rings. Use a spray to paint a fine transversal band around two-thirds of the log at the chosen disc positions.

(8) Marks on the bark. Use white correcting fluid to mark three points (**a**, **b**, and **c**) on the middle of each painted band. The points **a** and **c** should be roughly on opposite sides while **b** should lie on the top of the stem (Fig. 4). These points will be used to recover the spatial position of the disc. The mark **b** on the first disc should coincide with the stump mark.
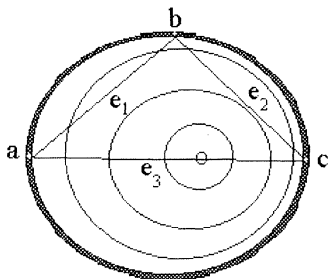

FIG. 4–Drawing represents the lower face of a wood disc (log large-end view) with the three marks and the measured distances on it.

(9) Measurements. Measure the distances $d_1, \ldots, d_6$ shown in Fig. 5 from the points **a**, **b**, and **c** on each wood disc to the corresponding levelling bolt ends.

(10) Crosscuts. Remove the device and proceed to cut the wood discs. Discs must contain the three marks and should be around 4 cm thick. Begin with the log large-end, and make a crosscut below the stump mark to obtain the lower face of the first disc. Once the first disc is cut, record the number 1 and the tree number on the upper face. The remaining discs are obtained similarly, recording on the upper face of each the disc and tree number.

(11) Additional measurements. Project the three marks **a**, **b**, and **c** of each disc on to its lower face, and measure the distances e_1, e_2, and e_3 as shown in Fig. 5. So far we have
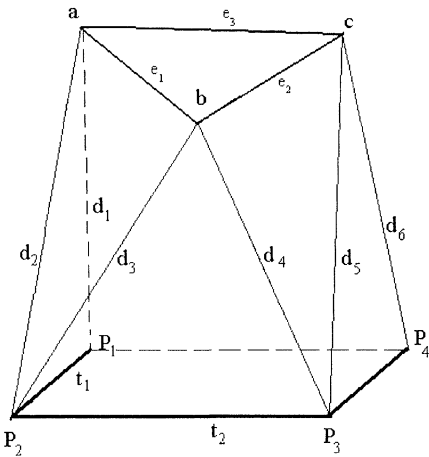
FIG. 5–The geometric body composed by all measurements.

nine distances for each disc: six of them correspond to measurements between the disc marks and the device, and the other three correspond to distances between the marks. These distances are sufficient to determine the co-ordinates of the points **a**, **b**, and **c** and to recover the spatial position of the wood disc.

COMPUTING THE SPATIAL CO-ORDINATES OF THE MARKS

The field procedure provides a number of distance measurements for each disc, namely $e_1, e_2, e_3, d_1, \ldots, d_6$. These distances may be used to set up a system of equations, which allows us to determine the Cartesian co-ordinates of the marks **a**, **b**, and **c** with respect to an appropriate co-ordinate system attached to the 3-DMD. To this end we consider a 3-D co-ordinate system with the origin placed at point P_2. The XY-plane is determined by the points P_1, P_2, P_3, and P_4 and while the Z-axis is given by the vertical direction. We choose the line passing through P_2 and P_3 as the X-axis, and the line through P_2 and P_1 as the Y-axis. In this reference frame the co-ordinates of the thin bolts are $P_1 = (0, t_1, 0)$, $P_2 = (0,0,0)$, $P_3 = (t_2, 0, 0)$, and $P_4 = (t_2, t_1, 0)$, where t_1 denotes the distance between P_1 and P_2, and t_2 the distance between P_2 and P_3. Similarly, the unknown co-ordinates of the marks in the disc are $P_a = (x_1, y_1, z_1)$, $P_b = (x_2, y_2, z_2)$, and $P_c = (x_3, y_3, z_3)$. In order to determine these nine unknowns we solve the system of equations $F(\bar{X}) = 0$ where $\bar{X} = (x_1, y_1, z_1, x_2, y_2, z_2, x_3, y_3, z_3)$ and the function $F(\bar{X})$ is given by

$$F(\bar{X}) = \begin{cases} x_1^2 + (y_1 - t_1)^2 + z_1^2 - d_1^2 \\ x_1^2 + y_1^2 + z_1^2 - d_2^2 \\ x_2^2 + y_2^2 + z_2^2 - d_3^2 \\ (x_2 - t_2)^2 + y_2^2 + z_2^2 - d_4^2 \\ (x_3 - t_2)^2 + y_3^2 + z_3^2 - d_5^2 \\ (x_3 - t_2)^2 + (y_3 - t_3)^2 + z_3^2 - d_6^2 \\ (x_1 - x_2)^2 + (y_1 - y_2)^2 + (z_1 - z_2)^2 - e_1^2 \\ (x_2 - x_3)^2 + (y_2 - y_3)^2 + (z_2 - z_3)^2 - e_2^2 \\ (x_3 - x_1)^2 + (y_3 - y_1)^2 + (z_3 - z_1)^2 - e_3^2 \end{cases}$$

This system of equations is solved by using Newton's method (Acton 1990), one of the most powerful and well-known numerical methods. To obtain an adequate starting point for

the iteration we suggest the following strategy to obtain a suitable initial point $\bar{X}_0$. First, notice that the unknowns y_1, x_2, and y_3 may be solved explicitly to obtain

$$y_1 = \frac{t_1}{2} + \frac{d_2^2 - d_1^2}{2t_1}, x_2 = \frac{t_2}{2} + \frac{d_3^2 - d_4^2}{2t_1}, y_3 = \frac{t_1}{2} + \frac{d_6^2 - d_5^2}{2t_1}.$$

Then, assuming as a first approximation that $z_1 = z_2 = z_3$ the last three equations become

$$(x_1 - x_2)^2 + (y_1 - y_2)^2 - e_1^2 = 0$$
$$(x_2 - x_3)^2 + (y_2 - y_3)^2 - e_2^2 = 0$$
$$(x_1 - x_3)^2 + (y_1 - y_3)^2 - e_3^2 = 0$$

which can be solved to obtain y_2, x_1, and x_3. Finally we get an approximation for the heights by taking $z_1 = \sqrt{d_2^2 - x_1^2 - y_1^2}$, $z_2 = \sqrt{d_3^2 - x_2^2 - y_2^2}$, and $z_3 \sqrt{d_5^2 - (t_2 - x_3)^2 - y_3^2}$. The point obtained in this way is close to the solution of the system and therefore it is a good initial point from which to start the application of Newton's method. As usual we stop the iterations by using a stopping rule of the form $\|F(\bar{X})\| \approx 0$.

The main error source in the proposed methodology may be attributed to the bending of the tape measure, especially on longer distances. We assume that this error is proportional to the distance — namely, if a distance d is measured, the error is rd where r is the error per unit length ($r \approx 1$ mm/m). We assume that the inaccuracies in the measurements e_1, e_2, e_3 as well as all other sources of error are negligible. In order to estimate the sensitivity of the solution $\bar{X}$ with respect to the errors in measurements, we assume that the disc has a sweep of s metres with respect to the vertical axis passing through the basis of the log. A first-order analysis provides the following bounds for the errors in the co-ordinates: in y_1, x_2, and y_3 a maximal error of $r(t_2 + 2s)$ mm; in y_2, x_1, and x_3 a maximal error of $2r(t_2 + 2s)$ mm; while for z_1, z_2, and z_3 the error is bounded by r times the maximum of $d_1,\ldots,d_6$. We remark that although the inaccuracy in the estimation of the heights z_i may be as large as 1 cm (on longer distances), their differences are still accurate to the millimetre (assuming that the bending effect is roughly the same on all measurements). This is important since it implies that the spatial orientation of the disc (i.e., the direction of the normal to its surface) is accurately recovered.

RING DATABASE

The data corresponding to the ring structure of each wood disc are obtained from a scanned image of the lower face of the disc (Fig. 6). This image contains four colours which correspond to the different kinds of data: white = background; black = ring border; red = marks **a**, **b**, and **c**; and green = approximate pith position.

A computer program extracts the positions of black pixels from the scanned image returning a 0–1 matrix (a 1 at position (i,j) corresponds to a black pixel). The indexes (i,j) corresponding to these 1's are used as local Cartesian co-ordinates to describe the position of the ring pixels relative to the pith. These co-ordinates are transformed into polar co-ordinates creating a database, which contains the angle and radius for each black pixel. We classify the angles into 180 discrete classes of 2 degrees each. For each particular angle class, we separate the rings into discrete classes by looking at the radial co-ordinates: if two pixels on the same angle class have radii which differ s units or more (s being an input constant) they are assigned to different rings. Every ring k is then described by 180 points of the form
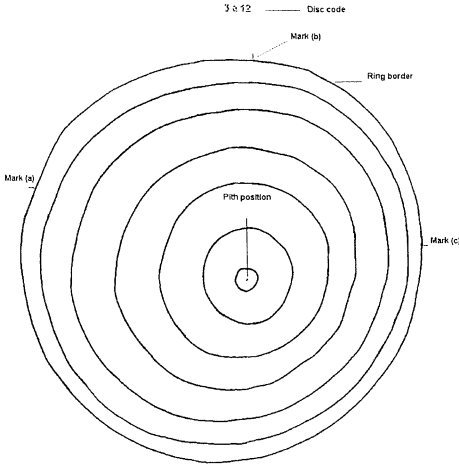
FIG. 6–A digital image of a disc obtained by scanning the disc face. Classifying angles and radii into discrete classes identifies the rings.

(θ_{kl}, r_{kl}) for $l = 1,...,180$, one for each angle class θ_{kl} and with radius r_{kl} equal to the average of the radii of pixels belonging to that ring in that particular angle class.

These ring data (θ_{kl}, r_{kl}) are transformed back into local Cartesian co-ordinates (x_{kl}, y_{kl}) relative to the pith position. Then, a simple linear transformation allows us to convert the latter into co-ordinates $(\alpha_{kl}, \beta_{kl})$ relative to a non-orthogonal reference frame with origin at point **b** and axis determined by the lines going through **ba** and **bc** (Fig. 7). Finally, the XYZ spatial co-ordinates of each point in the ring are obtained through the formula:

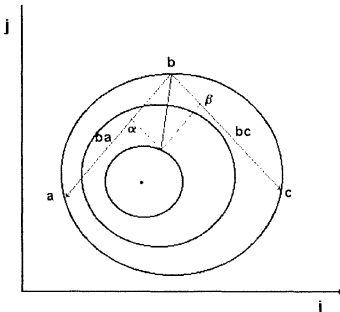$$P_{ki} = P_b + \alpha_{kl}(P_a - P_b) + \beta_{kl}(P_c - P_b).$$

FIG. 7–The local (α, β) co-ordinates of ring points.

APPLICATION:
RECONSTRUCTION OF A 10-YEAR-OLD *PINUS RADIATA* TREE

We present here an application of the proposed methodology, which concerns the study of deformations of *P. radiata* trees damaged by Pine Shoot Moth. This application allows us to look inside the tree structure and to reconstruct the annual development of the stem. In particular we may appreciate the specific changes inside the tree produced when a stem looses its verticality. Several other geometrical analyses may be done on the basis of the digital 3-D model of the log.

The specific example corresponds to a 10-year-old *P. radiata*. Using the proposed methodology we extracted 17 wood discs from the stem. In Fig. 8 can be seen the digital
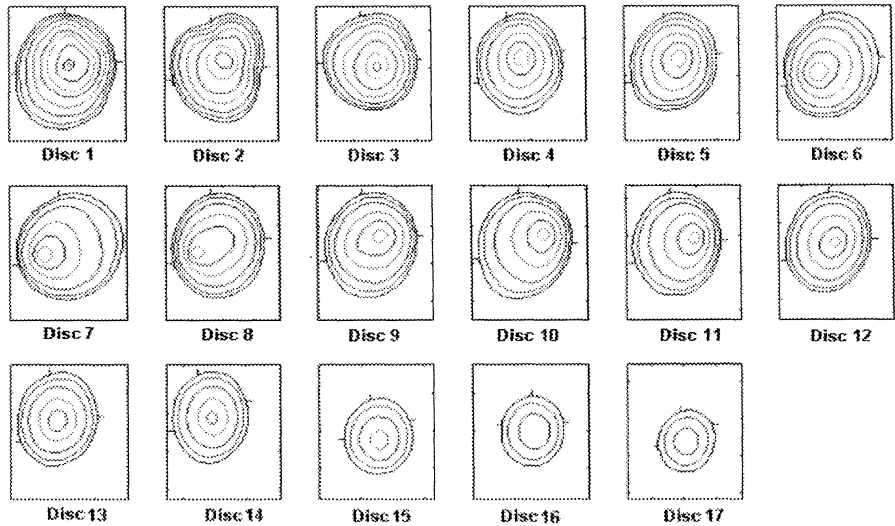
FIG. 8–The digital reconstruction of the 17 wood discs extracted from the pine tree. We can see the three position marks **a**, **b**, and **c**.

reconstruction and ring identification for all the discs. The original set of distance measurements for the disc marks **a**, **b**, and **c** are given in Table 1, and the XYZ co-ordinates of these marks as obtained by solving the corresponding system of equations are given in Table 2. Using these data we reconstruct the external and internal tree stem. To interpolate between the rings of neighbouring discs we use a cubic interpolator in such a way that the successive pieces fit smoothly. In Fig. 9 we show how to recover the shape of the stem along successive years, giving an idea of how the initial deformation evolved over time. Finally, in Fig. 10 we provide a view of the internal shape of the stem in the region near the maximal deformation.

The last 8 years of growth are shown in Fig. 9. The first 2 years are missing because they are located in the stump. We can observe each year of growth and the changes experienced by the tree.

In Fig. 10 we observe the annual rings (each one represented by a different shade of grey) and the position of the pith, represented as a black line in the inner ring. The nine transversal black lines indicate the disc positions, from Disc 4 (lower) to Disc 12 (upper). This image provides detailed information about the inner stem, diametrical growth, and eccentricities of the rings.

FINAL REMARKS

To improve precision in the reconstruction of the tree, especially for severe deformations, we suggest increasing the number of wood discs and using both faces of each disc.

The defect core position is relevant for pruned logs and it can also be included through the extraction of the stem sections containing the branch whorls. However, as the branches cause disturbances in the form of the growth rings, in the application above we avoided these stem portions in order to obtain clear rings without knots.

TABLE 1–Distances.

	Disc																
	1	2	3	4	5	6	7	8	9	10	11	12	13	14	15	16	17
D_1	44.6	87.2	103.8	127.1	136.1	142.2	148.6	158.1	158.1	161.9	165.5	171.5	185.9	273.7	381.8	520.5	610.5
D_2	61.1	100.9	114.9	136.9	145.3	151.2	157.1	165.8	165.8	169.2	172.5	178.6	192.9	277.7	384.1	522	612
D_3	62.6	101.2	114.4	136	144.9	149.7	155	161.8	161.8	166.9	173.4	179.5	192.2	276.9	384.5	522	611.8
D_4	61.2	102.7	114.8	136.4	145.1	150.7	155.7	160.5	160.5	164.6	171	178.1	191.6	276.8	385.4	522.5	612
D_5	59.7	101.1	113.9	136.3	145.3	151.2	154.4	157.6	157.6	163.4	172.2	180.1	192.5	277.8	385.4	522.5	611.3
D_6	44.1	88.2	102.8	128	137.4	143.4	146.7	150.5	150.5	156.4	166	173.8	186.3	274.5	383.4	521	610
E_1	11.4	10.1	8.8	9.9	10.2	11.2	11.2	11.2	11.2	10.8	11.0	11.5	10.2	8.4	6.8	6.1	5.7
E_2	9.9	10.1	10.6	9.6	9.9	10.6	11.7	10.7	10.7	10.3	9.8	9.2	9.4	8.6	6.8	6.1	5.3
E_3	15.4	14.3	14.9	13.7	14.2	15.5	16.5	15.6	15.6	14.8	14.2	14.1	12.5	12.2	10.7	9.7	8.9

Distances (cm)

TABLE 2–Position of the discs.

Units: cm

|		Disc																
		1	2	3	4	5	6	7	8	9	10	11	12	13	14	15	16	17
a	x_1	44.8	44.2	45.2	46.9	46.7	44.4	44.5	47.3	48.7	49.0	50.4	47.6	48.5	48.6	44.4	44.5	47.1
	y_1	42.6	50.7	49.4	50.9	50.9	51.6	51.1	50.2	49.7	49.3	48.7	49.9	51.6	47.3	42.7	41.0	43.5
	z_1	38.0	108.6	126.6	151.2	161.5	168.0	175.3	183.6	186.1	187.7	191.2	197.7	212.6	302.2	411.8	552.0	641.4
b	x_2	52.6	50.4	51.3	51.4	51.7	50.5	50.6	53.1	54.1	55.2	56.0	54.5	53.1	52.3	48.5	49.2	50.6
	y_2	34.5	42.8	43.0	42.1	42.1	42.2	41.8	40.8	40.7	40.5	39.3	40.8	42.5	39.8	37.3	37.1	39.0
	z_2	38.6	109.7	125.9	151.8	162.1	168.1	173.9	179.9	182.6	185.4	192.7	199.2	212.8	302.0	412.5	551.5	641.4
c	x_3	60.3	58.3	60.1	59.8	60.0	59.2	60.6	61.6	62.9	63.5	64.0	61.1	60.4	60.0	54.7	54.2	55.6
	y_3	41.0	49.0	48.8	46.7	47.1	47.7	48.0	46.8	46.3	47.3	45.7	47.0	48.2	43.2	40.1	40.6	40.7
	z_3	37.3	109.8	126.1	153.0	164.4	170.3	174.1	177.9	180.8	184.6	194.0	200.7	214.3	303.7	412.9	551.7	641.4
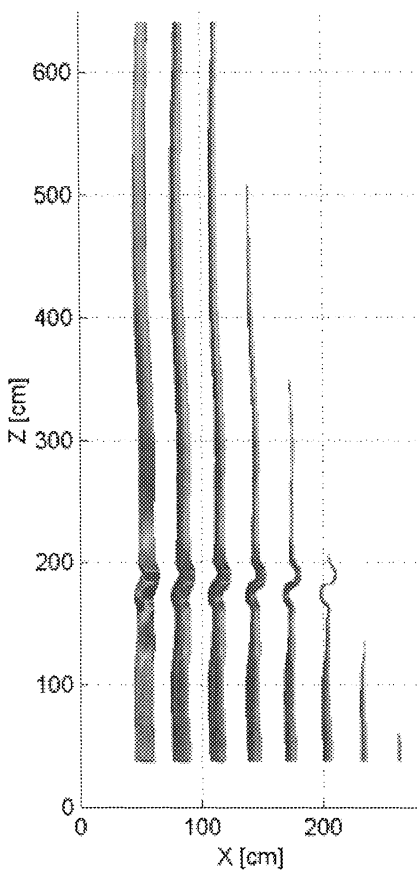
FIG. 9–The image represents the evolution
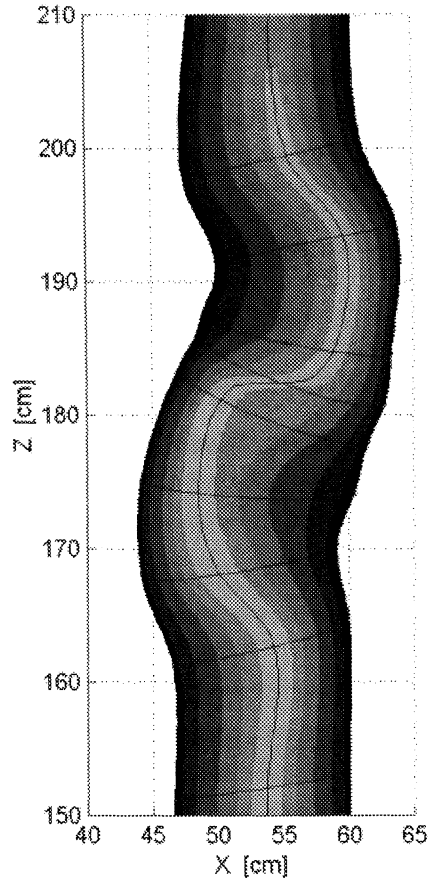of the tree during the last 8 years of
growth.

FIG. 10–Image shows a longitudinal cut
of the tree, between 155 and 210 cm
of height.

The methodology described in this article provides the data required to fit models for the development of deformations on trees and models related to ring form. On this matter, we mention here the model of ellipses developed by Saint-André & Leban (2000) and the growth ring model used in the sawing simulation software AUTOSAW (Todoroki 1997). In a forthcoming paper we will present a model for the deformation of trees based on considerations coming from the theory of elasticity. For a preliminary version see Padilla (2001).

In summary, the method presented can be used on straight or curved trees for stem analysis, volume tables, taper models, or to fit models related to stem and ring form. The use of the system on merchantable-size stems requires only scaling of the measuring device (3-DMD) to these sizes. The advantages of the proposed system, over similar methods, lie in its simplicity as well its great potential for calibrating models for log quality assessment based on ring information and internal defects such as knots (size and position).

ACKNOWLEDGMENTS

REFERENCES

ACTON, F. 1990: "Numerical Methods That Work". The Mathematical Association of America. 549 p.

BENSON-COOPER, D.M.; KNOWLES, R.L.; THOMPSON, F.J.; COWN, D.J. 1982: Computed tomographic scanning for the detection of defects within logs. *New Zealand Forest Service, FRI Bulletin No. 8.* 9 p.

BIRKELAND, R.; HOLOYEN, S. 1987: Industrial methods for internal scanning of log defects: A progress report on an ongoing project in Norway. *In* Proceedings of 2nd International Conference on Scanning Technology in Sawmills, 1–2 October, Oakland/Berkeley Hills, San Francisco.

ESPINOZA, H.; INOSTROZA, J. 1993: Informe final y evaluación del proyecto: Detección y control de la Polilla de Brote del Pino. Ministerio de Agricultura y Servicio Agrícola y Ganadero S.A.G. Santiago, Chile. 50 p.

FUNT, B.; BRYANT, E. 1987: Detection of internal log defects by automatic interpretation of computer images. *Forest Products Journal 37(1)*: 56–62.

HAN, W.; BIRKELAND, R. 1992: Ultrasonic scanning of logs. *Industrial Metrology 2(3–4)*: 253–282.

HARLESS, T.; WAGNER, F.; STEELE, P.; TAYLOR, F.; YADAMA, V.; McMILLIN, C. 1991: Methodology for locating defects within hardwood logs and determining their impact on lumber-value yield. *Forest Products Journal 41(4)*: 25–30.

HARRIS, J. 1991: Structure of wood and bark. Pp. 2-1 – 2-16 *in* Kininmonth, J.; Whitehouse, L.J. (Ed.) "Properties and Uses of New Zealand Radiata Pine. Vol. 1. Wood Properties". New Zealand Ministry of Forestry, Forest Research Institute, Rotorua.

HE, J. 1997: A comparison of artificial neuronal network classifiers for analysis of CT images for the inspection of hardwood logs. Thesis, Department of Electrical and Computer Engineering, Virginia Polytechnic Institute and State University. 86 p.

MORALES, S.; FERNÁNDEZ, P.; GUESALAGA, A.; IRARRÁZAVAL, P.: Proceedings of 4th Workshop: Connection between Forest Resources and Wood Quality: Modelling Approaches and Simulation Software. IUFRO, 8–15 September 2002, British Columbia, Canada (in press).

NIEMZ, P.; KUCERA, L. 1999: Possibility of defect detection in wood with ultrasound. *In* Proceedings of the Eleventh International Symposium on Nondestructive testing in Wood, 9–11 September, Madison, Wisconsin. United States.

OCEÑA, L.; SCHMOLDT, D. 1996: A prototype interactive graphic sawing program. *Forest Products Journal 46(11/12)*: 40–42.

PADILLA, F. 2001: Estudio de la recuperación de la deformación del fuste causada por Polilla del Brote *Rhyacionia buoliana* Den *et* Schiff. en *Pinus radiata* en la Décima Región. Tesis de Ingeniería Forestal, Facultad de Ciencias Forestales, Universidad de Chile. 127 p.

PARK, J.; LEMAN, C. 1983: A sawing study method for evaluating timber from pruned logs. *New Zealand Forest Service, FRI Bulletin No. 47.*

PETER, H.; BAMPING, J. 1962: Theoretical sawing of pine logs. *Forest Products Journal 12(11)*: 549–557.

PLOMION, C.; PIONNEAU, C.; BRACH, J.; COSTA, P.; BAILLÈRES, H. 2000: Compression wood-responsive proteins in developing xylem of Maritime Pine (*Pinus pinaster* Ait.). *Plant Physiology 123*: 959–969.

SAINT-ANDRÉ, L.; LEBAN, J.-M. 2000: An elliptical model for tree ring shape in transverse section. Methodology and case study on Norway Spruce. *Holz als Roh- und Werkstoff 58*: 368–374.

SCHMOLDT, D. 1996: CT imaging, data reduction and visualisation of hardwood logs. *In* Proceedings of the Twenty-fourth Annual Hardwood Symposium. High Hamton Cashiers, North Carolina, 8–11 May.

SCHMOLDT, D.; LI, P.; ARAMAN, P. 1995: A CT-based simulator for hardwood log veneering. Proceedings from the 2nd International Seminar/Workshop on Scanning Technology and Image Processing on Wood. Skelleftea, Sweden, 14–16 August.

SOMERVILLE, A. 1985: A field procedure for the cross-sectional analysis of a pruned radiata pine log. *New Zealand Forest Service, FRI Bulletin No. 101*.

SHAD, K.; SCHMOLDT, D.; ROSS, R. 1996: Nondestructive methods for detecting defects in softwood logs. U.S. Department of Agriculture, Forest Service, Forest Products Laboratory. 9 p.

STEELE, P.; WAGNER, F.; KUMAR, L.; ARAMAN, P. 1993: The value versus volume yield problem for live-sawn hardwood sawlogs. *Forest Products Journal 43(9)*: 35–40.

TODOROKI, C. 1997: Developments of the sawing simulation software, AUTOSAW: linking wood properties, sawing and lumber end-use. Pp. 241–247 *in* Proceedings of the Second Workshop IUFRO WP S5.01-04, 26–31 August, South Africa.

TSOUMIS, G. 1991: "Science and Technology of Wood. Structure, Properties, Utilisation". Van Nostrand Reinhold. New York. 494 p.

WANG, P.; CHANG, S. 1986: Nuclear magnetic resonance imaging of wood. *Wood and Fiber Science 18(2)*: 308–314.

ZHU, D.; CONNERS, R.; SCHMOLDT, D.; ARAMAN, P. 1996: A prototype vision system for analysing CT imagery of hardwood logs. IEEE Transactions on systems, man and cybernetics—Part B. *Cybernetics 26(4)*: 522–532.

ZIMMERMANN, M.; BROWN, C. 1971: "Trees: Structure and Function". Springer-Verlag. New York. 336 p.